Chem Biol Drug Des 2012

Research Article

Synthesis and Quantum Chemical Studies of New 4-aminoquinazoline Derivatives as Aurora A/B Kinase Inhibitors

Ming Zheng[1], Youguang Zheng[2], Yunsheng Xue[2], Yi Liu[2], Lin An[2], Ling Zhang[2], Min Ji[1,3,*], Bai Xue[1,4], Xuan Wu[2], Xuedong Gong[5], Ning Gu[1] and Xi Zhan[6]

[1]*School of Biological Science & Medical Engineering, Southeast University, Nanjing 211189, China*
[2]*School of Pharmacy, Xuzhou Medical College, Xuzhou 221004, China*
[3]*School of Chemistry & Chemical Engineering, Southeast University, Nanjing 211189, China*
[4]*JiangSu Simcere Pharmaceutical R&D Co., Ltd, Nanjing 210042, China*
[5]*Department of Chemistry, Nanjing University of Science and Technology, Nanjing 210094, China*
[6]*The Center for Inflammatory and Vascular Diseases, Department of Pathology, University of Maryland School of Medicine Baltimore, 800 West Baltimore Street, MD 21201, USA*
**Corresponding author: Min Ji, jimin@seu.edu.cn*
Ming Zheng and Youguang Zheng contributed equally to this work.

Nine novel 4-aminoquinazoline derivatives were designed and synthesized. Biochemical and cellular analyses demonstrated that most of the derivatives exhibited a strong activity to inhibit Aurora A and B kinases and to suppress the proliferation of a panel of human tumor cell lines (U937, K562, A549, LoVo, and HT29). Quantum chemical studies were also carried out to determine the structural features of these compounds engaged in the inhibition of Aurora kinases.

Key words: 4-aminoquinazolines, anti-proliferative activity, Aurora A and B, quantum chemistry

Received 30 July 2012, revised 7 October 2012 and accepted for publication 2 November 2012

Mammalian Aurora kinases constitute a small family of three closely related Ser/Thr kinases, named as Aurora A, B, and C. These kinases contain a highly conserved catalytic site and are involved in the progression of mitosis or meiosis, although the function of Aurora C is less understood (1,2). Aurora A localizes to the spindle poles and has a crucial role in the bipolar spindle formation (2). Aurora B is a chromosomal passenger protein and localizes at the centromeres during prometaphase and associates with midzone microtubules and midbodies during anaphase and telophase (1,3). Aurora C is specifically expressed in the testis and may play a role in spermatogenesis (4). The initial link between Aurora kinases and cancer was based on the observation that Aurora A and B were frequently overexpressed in colon cancer (5). Further studies found that Aurora A and B were overexpressed in a variety of solid tumors including prostate (6,7), pancreatic (8), breast (9), and thyroid cancers (10). Overexpression of Aurora A or B was mainly attributed to gene amplification and correlated with histological malignancy and poor prognosis (11). Recently, several small molecules with selective anti-Aurora activities have been developed and entered into preclinical or clinical trials for cancer treatment (12–14).

ZM447439 (AstraZeneca, Wilmington, DE), which has a 4-aminoquinazoline skeleton, was the first reported small inhibitor of Aurora kinases. *In vitro*, ZM447439 inhibits both Aurora A and B with IC_{50} values of 110 and 130 nM, respectively; impairs certain mitosis events, including chromosome alignment, chromosome segregation, and cytokinesis; and induces ultimately cell deaths (15,16). The report herein described our effort to improve the efficacy of inhibiting Aurora kinases by introducing an active imatinib group into several 4-aminoquinazoline analogs. This was achieved by intramolecular cyclization of the amide group on the benzene ring. We found that several new compounds generated by this approach have acquired improved potency in inhibiting both Aurora A and B kinases (Figure 1).

Methods and Materials

Chemistry

The strategy for synthesis of 4-aminoquinazoline derivatives is outlined in Scheme 1 (17). Interaction of cyclocondensation of 2-amino-4-fluorobenzoic acid **1** with formamidine acetate in the solvent of 2-methoxyethanol produced a high yield of compound **2**. Compound **2** was then treated with propylene glycol in the presence of sodium hydride to form compound **3**, which was further used to interact with thionyl chloride to generate chlorinated compound **4**. Using

 doi: 10.1111/cbdd.12089

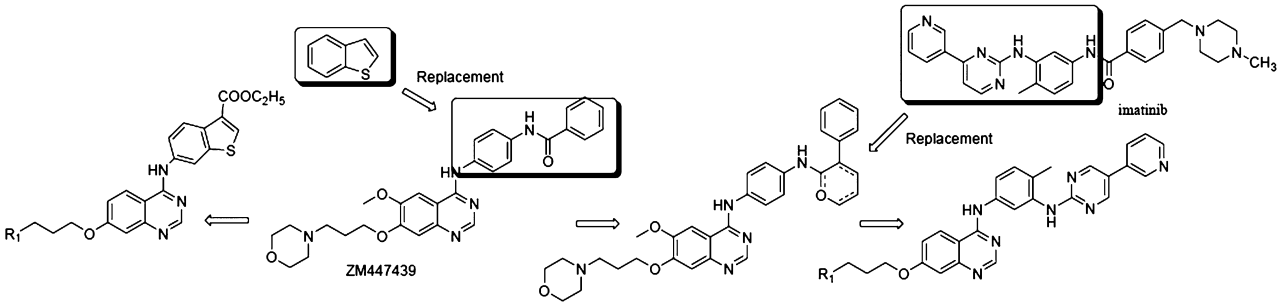

Figure 1: Design of the compounds.

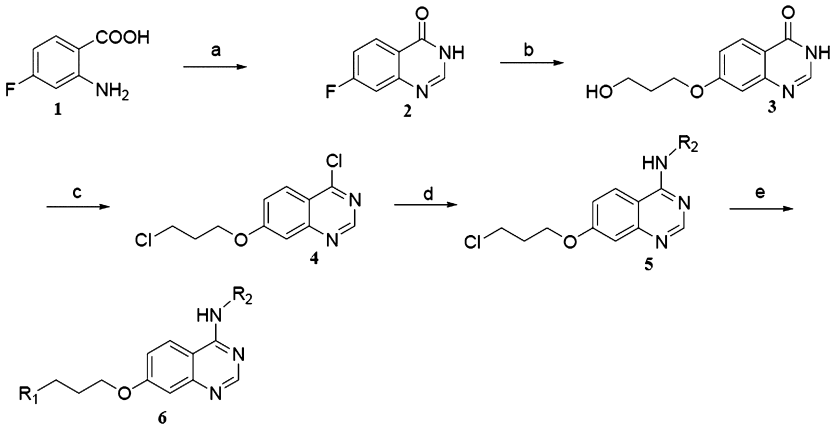

Scheme 1: Synthesis route of the Target Compounds. Reagents and conditions: a) Formamidine Acetate, 2-methoxyethanol; b) propylene glycol and NaH; c) SOCl2/DMF; d) aniline derivatives, isopropanol; e) secondary amine/DMF.

isopropanol as solvent, compound **4** reacted with aniline derivatives to yield 4-aminoquinazoline **5**, which furnished the final compound **6** upon treatment with the secondary amine in *N*, *N*-dimethylformamide.

Cell proliferation assay

The effect of the synthesized compounds on cell proliferation was assessed by MTT (Sigma-Aldrich Shanghai Trading Co Ltd Shanghai, China). The cell lines that were assessed include the following: U937 human acute monocytic leukemia cells, K562 human chronic myeloid leukemia cells, A540 human non-small cell lung cancer cells, and LoVo and HT29 human colon cancer cells. 5×10^3 cells were seeded in each well in a 96-well culture plate. The cell cultures were added with compounds to be tested at various concentrations in triplicates. Seventy-two hours later, the cell growth medium was removed, and each well was added with 5 mg/mL of MTT followed by incubation at 37 °C. After 4-h incubation, 50 μL of 20% SDS was added to each well, which was further incubated for overnight. Absorbance was measured with a plate reader at 570 nm with correction at 630 nm. The results were expressed as the percentage of absorbance of treated wells versus that of vehicle control. IC_{50}, the drug concentration causing 50% growth inhibition, was calculated via sigmoid curve fitting using GRAPHPAD PRISM 5.0 (GraphPad Software, Inc., La Jolla, CA, USA).

Aurora kinase assays

The kinase activity of Aurora A and B was measured using HTRF-KinEASE-STK discovery kit (Cisbio, Bedford, MA, USA). Briefly, Aurora A (65 nM) or Aurora B (316 nM) (Millipore, Billerica, MA, USA) was incubated with 1 μM STK substrate 2-biotin (Cisbio) and 15 μM ATP (Sigma-Aldrich) in the presence of tested compounds for 1 h at room temperature. The reaction was terminated by adding 200 mM EDTA. Phosphorylated substrates were incubated with STK antibody labeled with Eu^{3+}-cryptate and streptavidin-XL665. The Eu^{3+}-cryptate-conjugated antibody was excited at 340 nm, and cryptate and fluorescence resonance energy transfer emissions were detected at 615 and 665 nm, respectively. GRAPHPAD PRISM was used to generate IC_{50} values.

Quantum chemical calculation

The chemical structures of new compounds were drawn using HYPERCHEM 7.0 and optimized with its module of molecular mechanics (MM+ force field). The calculated structures at low energy were subjected to conformational analysis using HyperChem's Conformational Search module, and only those that have the most stable conformation were used in the next level of quantum chemical calculations. These calculations were performed using density functional theory (DFT) with the aid of GAUSSIAN03 software (Gaussian, Inc., Wallingford, CT, USA). B3LPY functional

and the 6-31G (d) basis set were used in the DFT calculations[b] (18–21). The fundamental vibrations were also calculated using the same method to determine whether they were true minima. The highest occupied molecular orbital (HOMO) and lowest unoccupied molecular orbital (LUMO) values, which were calculated as molecular orbital coefficients in artificial unit (a.u.), were converted into energy units in eV. The plots of HOMO and LUMO were generated using GAUSSVIEW 3.0 (Gaussian, Inc.).

Experimental Protocols

All reagents were purchased from commercial sources and used without further purification. Melting points were measured in open capillaries without correction. IR spectra were determined as KBr pellets on a Thermo Nicolet 6700 spectrophotometer. ^{1}H-NMR and ^{13}C-NMR spectra were recorded in DMSO-d_6 on a Bruker Avance 300 or 500 spectrometer; chemical shifts (δ) were reported in parts per million (ppm) relative to tetramethylsilane and used as an internal standard. Mass spectra (MS) were obtained from Agilent 1100LC/MS Spectrometry Services. Elementary analyses were performed on Elementar Vario EL III instrument. The purity of all compounds was routinely verified by TLC with silica gel GF-254 glass plates and viewed under UV light at 254 nm.

Compounds **6a–6i** were characterized as follows:

4-methyl-N^1-(7-(3-morpholinopropoxy)quinazolin-4-yl)-N^3-(5-(pyridin-3-yl)pyrimidin-2-yl)benzene-1,3-diamine(6a)

Yield 52.3%, mp 143 °C. IR (KBr, per cm): 3243.73, 2958.31, 2858.03, 1618.01, 1577.51, 1529.30, 1452.16, 1419.37, 1332.59, 1299.81, 1224.60, 1118.53, 1025.96, 794.54, 649.90; ^{1}H-NMR (DMSO-d_6, 300 MHz) δ (ppm): 1.90–1.97 (m, 2H, -CH_2-CH_2-CH_2-O-), 2.24 (s, 3H, –CH_3), 2.40 (m, 4H, 2 × morpholine-CH_2), 2.50 (m, 4H, 2 × morpholine-CH_2), 3.59 (s, 2H, -CH_2-CH_2-CH_2-O-), 4.20 (t, J = 6.06 Hz, 2H, -CH_2-CH_2-CH_2-O-), 7.14 (s, 1H, Ar-H), 7.25 (t, J = 8.31 Hz, 2H, Ar-H), 7.41–7.49 (m, 2H, Ar-H), 7.59 (d, J = 8.31 Hz, 1H, Ar-H), 8.13 (s, 1H, Ar-H), 8.43 (s, 2H, Ar-H), 8.52 (t, J = 2.91 Hz, 2H, Ar-H), 8.67 (d, J = 3.51 Hz, 2H, Ar-H), 8.98 (s, 1H, Ar-H), 9.28 (s, 1H, -NH-), 9.66 (s, 1H, -NH-); ^{13}C-NMR (DMSO-d_6, 75 MHz) δ (ppm): 17.61, 25.52, 53.20, 54.64, 66.01, 66.16, 107.41, 107.51, 109.30, 117.50, 118.71, 119.07, 123.65, 124.68, 127.54, 129.81, 132.12, 134.19, 137.28, 137.63, 148.11, 151.30, 151.94, 155.01, 157.37, 159.39, 161.16, 161.51, 161.88; ESI-MS m/z: 549.33 [M + H]$^+$.

4-methyl-N^1-(7-(3-(piperidin-1-yl)propoxy)quinazolin-4-yl)-N^3-(5-(pyridin-3-yl)pyrimidin-2-yl)benzene-1,3-diamine(6b)

Yield 52.1%, mp 170 °C. IR (KBr, per cm): 3423.08, 2944.82, 1618.01, 1577.51, 1523.51, 1452.16, 1413.59, 1334.52, 1297.88, 1224.60, 1132.03, 1002.82, 804.18, 651.83; ^{1}H-NMR (DMSO-d_6, 300 MHz) δ (ppm): 1.50 (m, 2H, -CH_2-CH_2-CH_2-O-),1.71 (s, 4H, 2 × piperidine-CH_2), 2.24 (s, 5H, -CH_3 and piperidine-CH_2), 2.95 (s, 4H, 2 × piperidine-CH_2), 3.33 (s, 2H, -CH_2-CH_2-CH_2-O-), 4.21 (s, 2H, -CH_2-CH_2-CH_2-O-), 7.22 (d, 3H, Ar-H), 7.42–7.56 (d, 3H, Ar-H), 8.13 (s, 1H, Ar-H), 8.43–8.51 (d, 4H, Ar-H), 8.66 (s, 1H, Ar-H), 8.98 (s, 1H, Ar-H), 9.28 (s, 1H, -NH-), 9.70 (s, 1H, -NH-); ^{13}C-NMR (DMSO-d_6, 75 MHz) δ(ppm): 17.61, 22.16, 23.18, 23.91, 52.52, 53.69, 65.70, 107.42, 107.67, 109.43, 117.35, 118.74, 119.10, 123.66, 124.78, 127.58, 129.81, 132.12, 134.20, 137.26, 137.62, 148.11, 151.31, 151.91, 155.05, 157.39, 159.40, 161.16, 161.51, 161.62; ESI-MS m/z: 547.3 [M + H]$^+$.

N^1-(7-(3-(diethylamino)propoxy)quinazolin-4-yl)-4-methyl-N^3-(5-(pyridin-3-yl)pyrimidin-2-yl)benzene-1,3-diamine(6c)

Yield 46.8%, mp 157 °C. IR (KBr, per cm): 3384.51, 2979.53, 2651.68, 1618.01, 1597.44, 1525.44, 1452.16, 1415.52, 1332.59, 1295.95, 1224.60, 1130.10, 1004.75, 987.39, 800.33, 707.76, 653.76; ^{1}H-NMR (DMSO-d_6, 300 MHz) δ (ppm): 1.89 (s, 2H, -CH_2-CH_2-CH_2-O-), 1.97–2.04 (d, 5H, diethylamine-CH_2-CH_3), 2.24 (s, 3H, -CH3), 2.78–2.87 (t, 5H, diethylamine-CH_2-CH_3), 3.98–4.05 (m, 2H, -CH_2-CH_2-CH_2-O-), 4.21 (s, 2H, -CH_2-CH_2-CH_2-O-), 7.15–7.24 (t, J = 7.05 Hz, 3H, Ar-H), 7.40–7.46 (t, J = 4.95 Hz, 2H, Ar-H), 7.59 (d, J = 7.74 Hz, 1H, Ar-H), 8.14 (s, 1H, Ar-H), 8.43 (s, 2H, Ar-H), 8.49–8.57 (dd, J_1 = 4.80 Hz, J_2 = 9.18 Hz, 2H, Ar-H), 8.66 (s, 1H, Ar-H), 8.99 (s, 1H, Ar-H), 9.28 (s, 1H, -NH-), 9.71 (s, 1H, -NH-); ^{13}C-NMR (DMSO-d_6, 75 MHz) δ(ppm): 7.78, 9.97, 14.04, 17.64, 20.71, 24.51, 46.26, 48.04, 58.56, 59.70, 65.71, 107.43, 107.58, 109.43, 117.53, 118.78, 119.14, 123.68, 124.84, 127.59, 129.82, 132.15, 134.22, 137.21, 137.64, 148.14, 151.33, 151.96, 155.07, 157.42, 159.42, 161.18, 161.53, 161.73; ESI-MS m/z: 535.34 [M + H]$^+$.

4-methyl-N^3-(5-(pyridin-3-yl)pyrimidin-2-yl)-N^1-(7-(3-(pyrrolidin-1-yl)propoxy)quinazolin-4-yl)benzene-1,3-diamine(6d)

Yield 31.5%, mp 125 °C. IR (KBr, per cm): 3423.08, 2960.24, 2805.96, 1618.01, 1577.51, 1529.30, 1454.09, 1419.37, 1334.52, 1297.88, 1224.60, 1130.10, 798.40, 705.83, 651.83; ^{1}H-NMR (DMSO-d_6, 500 MHz) δ(ppm): 1.68 (s, 4H, 2 × pyrrolidine-CH_2),1.90–1.98 (m, 2H, -CH_2-CH_2-CH_2-O-), 2.25 (s, 3H, -CH_3), 2.46–2.50 (m, 4H, 2 × pyrrolidine-CH_2), 2.59 (t, J = 7.15 Hz, 2H, -CH_2-CH_2-CH_2-O-), 4.17 (t, J = 6.35 Hz, 2H, -CH_2-CH_2-CH_2-O-), 7.15 (d, J = 2.45 Hz, 1H, Ar-H), 7.20–7.24 (m, 2H, Ar-H), 7.41 (d, J = 5.15 Hz, 1H, Ar-H), 7.45–7.47 (dd, J_1 = 4.80 Hz, J_2 = 4.75 Hz, 1H, Ar-H), 7.55–7.57 (dd, J_1 = 2.05 Hz, J_2 = 2.00 Hz, 1H, Ar-H), 8.13 (s, 1H, Ar-H), 8.41–8.44 (m, 2H, Ar-H), 8.46–8.51 (dd, J_1 = 9.25 Hz, J_2 = 5.10 Hz, 1H, Ar-H), 8.65–8.67 (dd, J_1 = 1.55 Hz, J_2 = 1.50 Hz, 1H, Ar-H), 8.96 (s, 1H, Ar-H), 9.28 (s, 1H,

-NH-), 9.59 (s, 1H, -NH-); ^{13}C-NMR (DMSO-d_6, 125 MHz) δ(ppm): 17.63, 23.06, 27.91, 52.08, 53.55, 66.25, 107.43, 107.52, 109.29, 117.54, 118.68, 119.04, 123.67, 124.58, 127.55, 129.85, 132.14, 134.20, 137.28, 137.67, 148.13, 151.32, 151.96, 155.04, 157.36, 159.41, 161.18, 161.53, 161.93; ESI-MS m/z: 533.32 [M + H]$^+$.

Ethyl 6-(7-(3-morpholinopropoxy)quinazolin-4-ylamino)benzo[b]thiophene-3-carboxylate(6e)

Yield 61.3%, mp 145 °C. IR (KBr, per cm): 3234.09, 2942.89, 1664.29, 1567.87, 1554.37, 1403.95, 1357.66, 1274.74, 1201.45, 1114.67, 958.46, 821.54; ^{1}H-NMR (DMSO-d_6, 500 MHz) δ(ppm): 1.36 (t, J = 7.15Hz, 3H, –CH_2-CH_3), 1.93–1.97 (dd, J_1 = 6.80 Hz, J_2 = 6.65 Hz, 2H, –CH_2-CH_3), 2.38 (s, 4H, 2 × morpholine-CH_2), 2.44–2.50 (dd, J_1 = 7.10 Hz, J_2 = 12.85 Hz, 2H, -CH_2-CH_2-CH_2-O-), 3.58 (t, J = 4.40 Hz, 4H, 2 × morpholine-CH_2), 4.19 (t, J = 6.30 Hz, 2H, -CH_2-CH_2-CH_2-O-), 4.34–4.38 (m, 2H, -CH_2-CH_2-CH_2-O-), 7.18 (d, J = 2.25 Hz, 1H, Ar-H), 7.24–7.26 (dd, J_1 = 2.00 Hz, J_2 = 2.00 Hz, 1H, Ar-H), 7.94–7.96 (dd, J_1 = 1.60 Hz, J_2 = 1.50 Hz, 1H, Ar-H), 8.04 (d, J = 8.80 Hz, 1H, Ar-H), 8.20 (s, 1H, Ar-H), 8.47–8.53 (m, 3H, Ar-H), 9.83 (s, 1H, -NH-); ^{13}C-NMR (DMSO-d_6, 125 MHz) δ(ppm): 14.12, 25.68, 53.33, 54.73, 61.39, 66.18, 66.26, 107.54, 109.29, 117.81, 118.25, 122.69, 123.52, 124.57, 130.74, 133.66, 136.41, 136.97, 138.80, 152.05, 154.52, 157.43, 161.97, 162.05; ESI-MS m/z: 493.22 [M + H]$^+$.

Ethyl 6-(7-(3-(4-methylpiperazin-1-yl)propoxy) quinazolin-4-ylamino)benzo[b]thiophene-3-carboxylate(6f)

Yield 43.7%, mp 162 °C. IR (KBr, per cm): 3274.59, 2937.10, 1712.51, 1619.94, 1577.51, 1529.30, 1450.23, 1413.59, 1292.09, 1230.38, 1149.38, 1072.24, 1014.39, 782.97, 754.04; ^{1}H-NMR (DMSO-d_6, 500 MHz) δ(ppm): 1.34 (t, J = 8.30 Hz, 3H, –CH_2-CH_3), 1.90–1.93(t, J = 6.20, 2H, –CH_2-CH_3), 2.18 (s, 4H, 2 × morpholine-CH_2), 2.40–2.49 (m, 9H, 2 × morpholine-CH_2, -CH_2-CH_2-CH_2-O- and –CH_3), 4.17 (d, J = 5.60 Hz, 2H, -CH_2-CH_2-CH_2-O-), 4.33–4.37 (m, 2H, -CH_2-CH_2-CH_2-O-), 7.15 (s, 1H, Ar-H), 7.24 (d, J = 8.85 Hz, 1H, Ar-H), 7.97 (d, J = 8.55 Hz, 1H, Ar-H), 8.03 (d, J = 8.70 Hz, 1H, Ar-H), 8.19 (s, 1H, Ar-H), 8.50–8.53 (m, 3H, Ar-H), 9.86 (s, 1H, -NH-); ^{13}C-NMR (DMSO-d_6, 125 MHz) δ(ppm): 14.10, 25.95, 45.31, 52.34, 54.15, 54.45, 61.36, 66.25, 107.50, 109.30, 117.74, 118.20, 122.63, 123.49, 124.63, 130.72, 133.62, 136.38, 137.00, 138.77, 152.03, 154.90, 157.42, 161.95, 162.02; ESI-MS m/z: 506.26 [M + H]$^+$.

Ethyl 6-(7-(3-(piperidin-1-yl)propoxy)quinazolin-4-ylamino)benzo[b]thiophene-3-carboxylate(6g)

Yield 57.9%, mp 170–171 °C. IR (KBr, per cm): 3390.58, 2933.73, 1709.27, 1619.05, 1570.93, 1526.82, 1454.64, 1410.53, 1228.07, 1127.82, 1069.67, 1053.63, 756.89; ^{1}H-NMR (DMSO-d_6, 300 MHz) δ(ppm): 1.32–1.39 (m, 5H, –CH_2-CH_3), 1.50 (d, 4H, 2 × piperidine-CH_2), 1.93 (t, J = 6.96 Hz, 2H, -CH_2-CH_2-CH_2-O-), 2.34–2.44 (m, 6H, 3 × piperidine-CH_2), 4.18 (t, J = 6.33 Hz, 2H, -CH_2-CH_2-CH_2-O-), 4.32–4.39 (m, 2H, -CH_2-CH_2-CH_2-O-), 7.17 (d, J = 2.37 Hz, 1H, Ar-H), 7.24–7.27 (dd, J_1 = 2.37 Hz, J_2 = 2.37 Hz, 1H, Ar-H), 7.93–7.97 (d, J_1 = 1.98 Hz, J_2 = 1.86 Hz, 1H, Ar-H), 8.03 (d, J = 8.82 Hz, 1H, Ar-H), 8.21 (s, 1H, Ar-H), 8.47–8.53 (m, 3H, Ar-H), 9.85 (s, 1H, -NH-); ^{13}C-NMR (DMSO-d_6, 125 MHz) δ(ppm): 14.11, 24.10, 25.57, 26.10, 54.07, 55.00, 61.38, 66.42, 107.53, 109.26, 117.82, 118.26, 122.69, 123.54, 124.56, 130.74, 133.65, 136.41, 138.79, 152.05. 154.91, 157.42, 161.96, 162.08; ESI-MS m/z: 491.4 [M + H]$^+$.

Ethyl 6-(7-(3-(pyrrolidin-1-yl)propoxy)quinazolin-4-ylamino)benzo[b]thiophene-3-carboxylate(6h)

Yield 36.9%, mp 170 °C. IR (KBr, per cm): 3426.94, 2964.10, 2875.39, 2788.61, 1618.01, 1575.58, 1519.66, 1456.02, 1432.58, 1417.45, 1338.38, 1230.38, 1130.10, 81.32, 717.40, 676.90; ^{1}H-NMR (DMSO-d_6, 300 MHz) δ(ppm): 1.85–2.00 (m, 5H, –CH_2-CH_3), 2.49–2.54 (m, 4H, 2 × pyrrolidine-CH_2), 2.65 (t, J = 6.93 Hz, 2H, -CH_2-CH_2-CH_2-O-), 3.51–3.55 (t, 4H, 2 × pyrrolidine-CH_2), 3.85 (d, J = 6.15 Hz, 2H, -CH_2-CH_2-CH_2-O-), 4.20 (t, J = 6.27 Hz, 2H, -CH_2-CH_2-CH_2-O-), 7.17 (d, J = 2.43 Hz, 1H, Ar-H), 7.23–7.27 (dd, J_1 = 2.43 Hz, J_2 = 2.43 Hz, 1H, Ar-H), 7.81–7.84 (dd, J_1 = 2.07 Hz, J_2 = 1.92 Hz, 1H, Ar-H), 7.96–8.02 (dd, J_1 = 5.10 Hz, J_2 = 11.91 Hz, 2H, Ar-H), 8.49–8.62 (m, 3H, Ar-H), 10.02 (s, 1H, -NH-); ^{13}C-NMR (DMSO-d_6, 125 MHz) δ(ppm): 22.96, 23.51, 26.15, 27.19, 47.25, 48.47, 51.86, 53.45, 66.01, 107.61, 109.37, 113.64, 117.69, 117.87, 118.37, 122.12, 123.11, 124.65, 125.14, 134.80, 136.54, 139.64, 140.58, 152.01, 154.97, 155.60, 157.55, 160.79, 161.92; ESI-MS m/z: 477.2 [M + H]$^+$.

Ethyl 6-(7-(3-(diethylamino)propoxy)quinazolin-4-ylamino)benzo[b]thiophene-3-carboxylate(6i)

Yield 35.7%, mp 160 °C. IR (KBr, per cm): 3455.87, 3025.81, 2971.81, 2933.24, 2802.11, 1706.72, 1618.01, 1577.51, 1526.27, 1450.23, 1409.73, 1326.81, 1172.53, 1149.38, 1130.10, 1070.32, 1020.18, 912.18, 755.97, 674.97; ^{1}H-NMR (DMSO-d_6, 300 MHz) δ(ppm): 0.89–0.97 (m, 6H, 2 × diethylamine-CH_3), 1.28–1.37 (m, 3H, –CH_2-CH_3), 1.85–1.91 (dd, J_1 = 6.54 Hz, J_2 = 5.12 Hz, 2H, -CH_2-CH_2-CH_2-O-), 2.42–2.57 (m, 6H, 2 × diethylamine-CH_2 and –CH_2-CH_3), 4.17(t, J = 6.12 Hz, 2H, -CH_2-CH_2-CH_2-O-), 4.32–4.39 (t, 2H, -CH_2-CH_2-CH_2-O-), 7.16 (s, 1H, Ar-H), 7.26 (d, J = 9.03 Hz, 1H, Ar-H), 7.97 (d, J = 8.91 Hz, 1H, Ar-H), 8.05 (d, J = 8.76 Hz, 1H, Ar-H), 8.20 (s, 1H, Ar-H), 8.47–8.53 (m, 3H, Ar-H), 9.86 (s, 1H, -NH-); ^{13}C-NMR (DMSO-d_6, 125 MHz) δ(ppm): 11.83, 14.09, 26.45, 46.42, 48.57, 61.35, 66.23, 107.46, 109.27, 117.76, 118.20, 122.63, 123.48, 124.56, 130.71, 133.63, 136.38, 137.00, 138.77, 139.36, 152.05, 154.87, 157.41, 161.94, 162.10; ESI-MS m/z: 479.4 [M + H]$^+$.

Results and Discussion

Analysis of the inhibitory activity of new compounds against Aurora A/B kinases

We have synthesized nine compounds derived from 4-aminoquinazoline. To explore the mechanism of action of these new compounds, they were analyzed for the inhibition of Aurora A/B kinases. As shown in Table 1, most of the derivatives exhibit a higher selectivity for Aurora A than Aurora B. For example, compound **6d** has a lower IC_{50} value (77 nM) for Aurora A than that for Aurora B (144 nM). Introduction of the active group of imatinib at the amine of C-4 of the quinazoline ring in compounds **6a–6d** improved the inhibitory activity as compared to aniline analogs **6e–6i**. To facilitate structure–activity relationship (SAR) analysis, we maintained the aniline group at R2 while varying the side chain substituent at R1. We found that variations of the secondary amine substituent at R1 also resulted in dramatic changes in the inhibition of Aurora kinases. Compounds **6d** and **6h** with a pyrrole side chain showed the strongest inhibitory activity. Compounds **6b** and **6g** with a piperidine were significantly less potent than that of **6d** and **6h**. Compound **6a** with a morpholine at R1 had also a modest activity to inhibit Aurora kinases. However, compound **6e**, which has a similar side chain, did not show a detectable activity against Aurora A/B. Replacement of the pyrrole group in compound **6d** with diethylamine group did not change the anti-Aurora activity (**6c**). On the other hand, the similar replacement in **6h** led to a significant reduction in the potency (**6i**). Compound **6f**, which has an *N*-methyl piperazine at R1, exhibited a similar activity as ZM447439. Thus, changes in R1 and R2 side chains of 4-aminoquinazoline can improve the potency against Aurora kinases.

Table 1: Aurora A/B inhibitory activity of 4-aminoquinazoline derivates

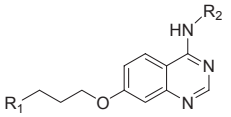

Compound	R_1	R_2	IC_{50}(nM)[a] Aurora A	Aurora B
6a		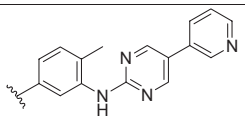	179	191
6b		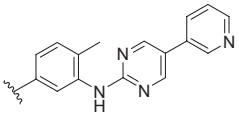	323	489
6c		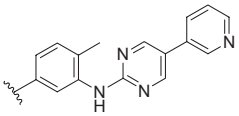	98	202
6d		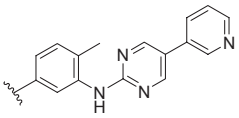	77	145
6e		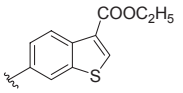	NT	NT
6f	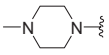	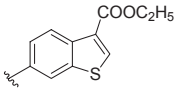	111	136
6g		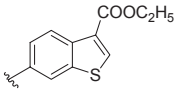	822	NT
6h		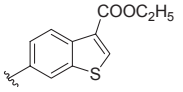	62	146
6i		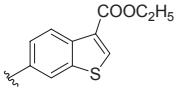	788	893
ZM447439			138	156

NT, not tested.
[a]The mean of at least two experiments.

Analysis of antiproliferation activity

All the new compounds were evaluated for the potential to inhibit the growth of human tumor cells. For this purpose, we chose five cell lines representing different tumor types, including human acute monocytic leukemia cell line (U937), human chronic myeloid leukemia cell line (K562), human non-small cell lung cancer (A549), and human colon cancer (LoVo and HT29). The result of the study was summarized in Table 2. Most of the compounds had evident antiproliferation effect on solid tumor cell lines (A549, LoVo, and HT29) but poor effect on leukemia cells (U937 and K562). In particular, compounds **6c** and **6d** have IC_{50} values ranging from 0.99 to 4.35 μM toward solid tumor cells, which are similar to or better than that of ZM447439 (IC_{50} = 1.87–3.36 μM). In addition, compounds **6c** and **6d** also showed increased potency against leukemia cell lines as compared to ZM447439. We proposed that the higher cytotoxicity of these compounds could be attributed to the active group of imatinib substituted at the R2 side chain. Indeed, compound **6b**, which has the same active group, also showed a similar activity against solid tumor cell lines with an IC_{50} value of 2.01–2.85 μM. Also compound **6g**, which has a R1 side chain (piperidine) same as **6b** but has an aniline group at R2, exhibited a significant decrease in the cytotoxic activity (IC_{50} > 100 μM for the most tumor cells) and poor potency against Aurora A/B kinases. On the other hand, compounds **6d** and **6h,** which have a pyrrolidine ring at the R1 side chain but with different R2 groups, inhibited the growth of solid tumor cells with IC_{50} values from 1.98 to 5.44 μM. Thus, the side chain at R1 also has a significant impact on the antiproliferation activity. Another interesting observation is that compound **6f**, which has an *N*-methyl piperazine at R1 and a similar anti-Aurora kinase activity as ZM447439, was more potent than ZM447439 in inhibiting tumor cell growths. This difference may be

Table 2: *In vitro* cytotoxic activity of target compounds against cancer cells

Compound	IC_{50} (μM)[a]				
	U937	K562	A549	LoVo	HT29
6a	>100	>100	>100	6.09	9.90
6b	11.30	>100	2.85	2.20	2.01
6c	7.20	4.00	0.99	1.65	4.35
6d	4.90	2.00	2.85	1.98	1.99
6e	>100	>100	6.23	5.88	2.16
6f	4.90	2.00	2.26	1.21	1.89
6g	>100	>100	>100	6.88	>100
6h	10.60	>100	2.53	5.44	4.26
6i	>100	>100	8.85	7.35	>100
ZM447439	>100	>100	3.36	1.87	2.23

[a]Cellular proliferation was determined by MTT assay.

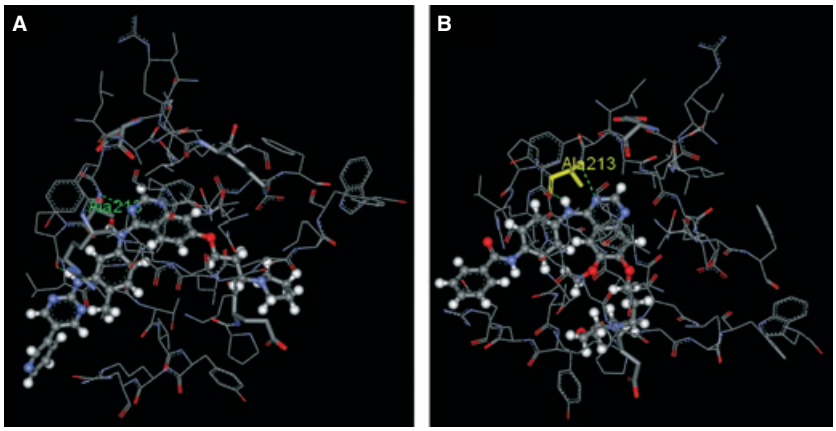

Figure 2: (A) Binding mode of compounds **6d** with Aurora A; (B) Binding interaction of ZM-447439 with Aurora A.

due to different permeability of these two compounds into cells.

Molecular docking analysis

The coordinate for the Aurora A structure was obtained from the RCSB Protein Data Bank (PDB ID: 2NP8). The protein structure was presented using SYBYL 7.3 software (Tripos International, St. Louis, MO, USA) and subjected to molecular modeling, which indicates that compound **6d** would dock strongly into the ATP-binding site of Aurora A (Figure 2A). It also reveals that the compound participates in a hydrogen bond interaction with the amine group of Ala213 within the protein hinge region (Figure 2A). Interestingly, the

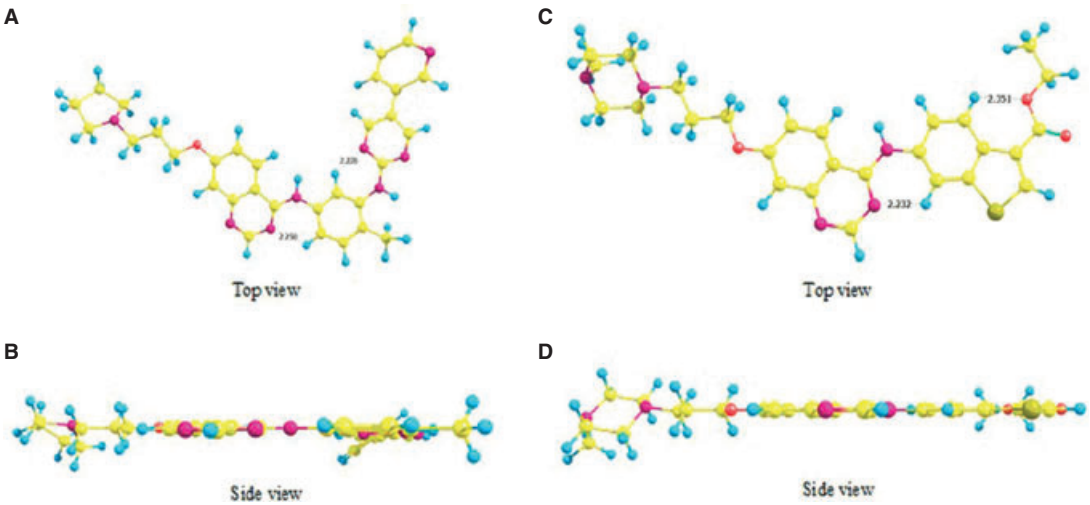

Figure 3: The optimized structures of the most active compounds **6d** (A, B) and **6f** (C, D).

amine between benzene and pyrimidine ring also makes a hydrogen bond to the hinge region of the kinase, which is apparently absent in the binding mode of ZM 447439 with Aurora A (Figure 2B). We proposed that this extra hydrogen bond may contribute to the apparent high activity of compound **6d** to inhibit Aurora kinases and cell growth.

Quantum chemical studies

To gain further insight into the structural basis for these compounds to interact with their targets, conformational analysis was performed using MM+ force field in HYPERCHEM 7.0[a]. The analysis demonstrated that the lowest energy-minimized structures of compounds **6a–d** take a coplanar configuration of the benzopyrimidine, benzene, and pyrimidine moieties. Such configuration is apparently stabilized by intramolecular hydrogen bond between the CH group in the benzene ring and the adjacent nitrogen atom in the pyrimidine ring (Figure 3A, B). The compounds **6a–c** have a structure similar to **6d**. As for compounds **6e–i**, their benzopyrimidine and benzothiophene moieties are also configured into a structural plane (Figure 3C, D).

It has been reported that molecular electronic effects play a critical role in controlling the pharmacological activities of drugs (22). In SAR analysis, quantum chemical parameters have yielded promising estimation for the correlation of the electronic effects with the biological activity (23–25). These parameters include the HOMO and the LUMO (26), which reflect the frontier molecular orbitals that dominate the reactivity of a molecule. Thus, we calculated the orbital energies of both HOMO and LUMO and their gaps for all the new compounds, the result of which is presented in Table 3. Significantly, we observed that compounds **6d** and **6f** have the lowest energy gap (ΔE) of 4.0115 and 3.9426 eV, respectively, and both exhibit the highest cytotoxic activity.

We also plotted the HOMO and LUMO of these compounds to analyze the atomic contributions of these orbitals to the sites for electronic transfer between individual compound and its biological target. As the representatives, the plots of the HOMO and LUMO of the most active compounds (**6d** and **6f**) are presented in Figure 4. The results illustrate that the HOMO molecular orbital of **6d** is mainly located in the benzopyrimidine, benzene, and pyrimidine moieties, indicative of the existence of possible reactive sites that may be involved in electrophilic attacks. On the other hand, the LUMO of **6d** is primarily concentrated on pyridine and pyrimidine rings in which the negatively charged polar residues of the receptor may be

Table 3: Energies of both HOMO and LUMO and their gaps (in eV) calculated for all compounds

Compound	E_{HOMO} (eV)	E_{LUMO} (eV)	ΔE (eV)
6a	−5.36205	−1.34126	4.020786
6b	−5.33647	−1.32493	4.011534
6c	−5.33783	−1.32520	4.012623
6d	−5.33538	−1.32384	4.011534
6e	−5.56205	−1.54507	4.016976
6f	−5.46627	−1.52358	3.942689
6g	−5.53484	−1.51024	4.024596
6h	−5.53321	−1.50834	4.024868
6i	−5.53647	−1.51052	4.025956

HOMO, highest occupied molecular orbital; LUMO, lowest unoccupied molecular orbital.

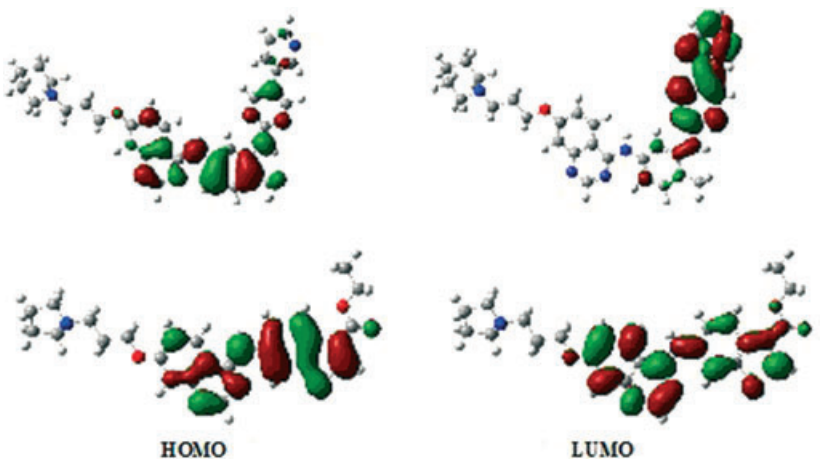

Figure 4: Plots of the highest occupied molecular orbital (HOMO) and lowest unoccupied molecular orbital (LUMO) of the most active compounds **6d** (upper) and **6f** (lower).

favorable. When compared with **6d**, the HOMO and LUMO of **6f** are quite similar and delocalized in benzopyrimidine and benzothiophene moieties.

Conclusion

We have designed a series of 4-aminoquinazoline derivatives and analyzed their anti-Aurora kinase activities. Most of the compounds showed a significant antiproliferation activity against three solid tumor cell lines, but no or poor activity against two leukemia cell lines. Introduction of the active group of imatinib at the R2 side chain or a pyrrolidine ring at the R1 side chain impacts significantly the activity for both anti-Aurora kinases and antigrowth of tumor cells. Molecular modeling suggested that the strong inhibitory activity of compound **6d** may be attributed to an extra hydrogen bond between the amine at the pyrimidine ring and the hinge region of targeted kinases. Quantum chemical calculation of electronic parameters including HOMO and LUMO indicates an association of molecular orbitals at low energy with antiproliferation activities of these compounds. These findings may be useful in improving the efficacy of Aurora A/B kinase inhibitors by incorporating some structural groups that are able to modify the electronic property of the existing anti-Aurora compounds.

Acknowledgments

This work was supported by National Basic Research Program of China (No. 2011CB933503), 'Qing-Lan' Project of Jiangsu Province; The National Natural Science Foundation of China (No. 81202490); Natural Science Foundation of Jiangsu Province (BK2009253); The Industrialization of Scientific Research Promotion Projects of Colleges and Universities in Jiangsu Province (JHZD09-23); Natural Science Fund for Colleges and Universities in Jiangsu Province (09KJB350003; 11KJB350005); and Science and Technology Project of Xuzhou, China (XZZD1224); The authors are grateful for these financial supports.

References

1. Carmena M., Earnshaw W.C. (2003) The cellular geography of Aurora kinases. Nat Rev Mol Cell Biol;4:842–854.
2. Marumoto T., Zhang D., Saya H. (2005) Aurora-A – a guardian of poles. Nat Rev Cancer;5:42–50.
3. Kimura M., Matsuda Y., Yoshioka T., Sumi N., Okano Y. (1998) Identification and characterization of STK12/Aik2: a human gene related to aurora of Drosophila and yeast IPL1. Cytogenet Cell Genet;82:147–152.
4. Tang C.J., Lin C.Y., Tang T.K. (2006) Dynamic localization and functional implications of Aurora-C kinase during male mouse meiosis. Dev Biol;290:398–410.
5. Bischoff J.R., Anderson L., Zhu Y., Mossie K., Ng L., Souza B., Schryver B., Flanagan P., Clairvoyant F., Ginther C., Chan C.S., Novotny M., Slamon D.J., Plowman G.D. (1998) A homologue of Drosophila Aurora kinase is oncogenic and amplified in human colorectal cancers. EMBO J;17:3052–3065.
6. Chieffi P., Cozzolino L., Kisslinger A., Libertini S., Staibano S., Mansueto G., De Rosa G., Villacci A., Vitale M., Linardopoulos S., Portella G., Tramontano D. (2006) Aurora B expression directly correlates with prostate cancer malignancy and influence prostate cell proliferation. Prostate;66:326–333.
7. Ewart-Toland A., Dai Q., Gao Y.T., Nagase H., Dunlop M.G., Farrington S.M., Barnetson R.A. *et al.* (2005) Aurora-A/STK15 T + 91A is a general low penetrance cancer susceptibility gene: a meta-analysis of multiple cancer types. Carcinogenesis;26:1368–1373.
8. Li D., Zhu J., Firozi P.F., Abbruzzese J.L., Evans D.B., Cleary K., Friess H., Sen S. (2003) Overexpression of oncogenic STK15/BTAK/Aurora A kinase in human pancreatic cancer. Clin Cancer Res;9:991–997.
9. Tanaka T., Kimura M., Matsunaga K., Fukada D., Mori H., Okano Y. (1999) Centrosomal kinase AIK1 is overexpressed in invasive ductal carcinoma of the breast. Cancer Res;59:2041–2044.
10. Ulisse S., Delcros J.G., Baldini E., Toller M., Curcio F., Giacomelli L., Prigent C., Ambesi-Impiombato F.S., D'Armiento M., Arlot-Bonnemains Y. (2006) Expression of Aurora kinases in human thyroid carcinoma cell lines and tissues. Int J Cancer;119:275–282.
11. McLaughlin J., Markovtsov V., Li H., Wong S., Gelman M., Zhu Y., Franci C. *et al.* (2010) Preclinical characterization of Aurora kinase inhibitor R763/AS703569 identified through an image-based phenotypic screen. J Cancer Res Clin Oncol;136:99–113.
12. Harrington E.A., Bebbington D., Moore J., Rasmussen R.K., Ajose-Adeogun A.O., Nakayama T., Graham J.A., Demur C., Hercend T., Diu-Hercend A., Su M., Golec J.M.C., Miller K.M. (2004) VX-680, a potent and selective small-molecule inhibitor of the Aurora kinases, suppresses tumor growth in vivo. Nat Med;10:262–267.
13. Manfredi M., Ecsedy J., Meetze K., Balani S., Burenkova O., Chen W., Hoar K. *et al.* (2006) 97th Annual AACR Meeting, Washington, DC, Abstract 4724.
14. Wilkinson R.W., Keen N., Odedra R., Heaton S.P., Wedge S.R., Foote K.M., Mortlock A., Jung F., Heron N.M., Brady M.C., Walker M., Khatri L., Barrass N.C., Foster J.J., Green S. (2006) 97th Annual AACR Meeting, Washington, DC, Abstract 5673.
15. Ditchfield C., Johnson V.L., Tighe A., Ellston R., Haworth C., Johnson T., Mortlock A., Keen N., Taylor S.S. (2003) Aurora B couples chromosome alignment with anaphase by targeting BubR1, Mad2, and Cenp-E to kinetochores. J Cell Biol;161:267–280.
16. Gadea B.B., Ruderman J.V. (2005) Aurora kinase inhibitor ZM447439 blocks chromosome-induced spindle assembly, the completion of chromosome condensation, and the establishment of the spindle integrity checkpoint in Xenopus egg extracts. Mol Biol Cell;16:1305–1318.

17. Mortlock A.A., Foote K.M., Heron N.M., Jung F.H., Pasquet G., Lohmann J.J., Warin N. *et al.* (2007) Discovery, synthesis, and in vivo activity of a new class of pyrazoloquinazolines as selective inhibitors of Aurora B kinase. J Med Chem;50:2213–2224.
18. Becke A.D. (1988) Density-functional exchange-energy approximation with correct asymptotic behavior. Phys Rev A;38:3098–3100.
19. Lee C., Yang W., Parr R.G. (1988) Development of the Colle-Salvetti conelation energy formula into a functional of the electron density. Phys Rev B Condens Matter;37:785–789.
20. Parr R.G., Yang W. (1989) Density-functional Theory of Atoms and Molecules. New York: Oxford University Press.
21. Becke A.D. (1993) Density-functional thermochemistry. III. The role of exact exchange. J Chem Phys;98:5648–5652.
22. Matysiak J. (2007) Evaluation of electronic, lipophilic and membrane affinity effects on antiproliferative activity of 5-substituted-2-(2,4-dihydroxyphenyl)-1,3,4- thiadiazoles against various human cancer cells. Eur J Med Chem;42:940–947.
23. Schon U., Antel J., Bruckner R., Messinger J., Franke R., Gruska A. (1998) Synthesis, pharmacological characterization, and quantitative structure-activity relationship analyses of 3,7,9,9- tetraalkylbispidines: derivatives with specific bradycardic activity. J Med Chem;41:318–331.
24. Roy D.R., Pal N., Mitra A., Bultinck P., Parthasarathi R., Subramanian V., Chattaraj P.K. (2007) An atom counting strategy towards analyzing the biological activity of sex hormones. Eur J Med Chem;42:1365–1369.
25. Raya A., Barrientos-Salcedo C., Rubio-Póo C., Soriano-Correa C. (2011) Electronic structure evaluation through quantum chemical descriptors of 17β-aminoestrogens with an anticoagulant effect. Eur J Med Chem;46:2463–2468.
26. Fukui K. (1982) Role of frontier orbitals in chemical reactions. Science;218:747–754.

Notes

[a](2002) HyperChem (Molecular Modeling System) Hypercube, Inc., Gainesville, FL, USA.

[b]Frisch M.J., Trucks G.W., Schlegel H.B., Scuseria G.E., Robb M.A., Cheeseman J.R., Montgomery J.A., Vreven Jr. T., Kudin K.N., Burant J.C., Millam J.M., Iyengar S.S., Tomasi J., Barone V., Mennucci B., *et al.* (2004) Gaussian 03, Revision D.01, Gaussian, Inc., Wallingford CT.